

**GREEN SYNTHESIS OF SILVER NANOPARTICLES USING NIGERIAN PROPOLIS EXTRACT FOR ENHANCED CORROSION PROTECTION OF CARBON STEEL IN ACIDIC ENVIRONMENTS**

**Author Details:**

**Dr. Olamide T. Nwazobi**

**Department of Chemical Engineering, Federal University of Technology, Minna, Nigeria**

**Dr. Nafisa E. Akerinde**

**Department of Chemistry, University of Ilorin, Ilorin, Nigeria**

**Dr. Ibrahim M. Chukwudozie**

**Materials Science Division, African Institute of Science and Technology, Abuja, Nigeria**

**Dr. Ijeoma K. Onuorah**

**Centre for Nanotechnology and Advanced Materials, University of Nigeria, Nsukka**

**VOLUME01 ISSUE01 (2024)**

Published Date: 14 December 2024 // Page no.: - 27-35

---

**ABSTRACT**

The relentless corrosion of carbon steel, especially within the harsh acidic conditions of many industries, presents significant economic and safety challenges. In response, this study explores a sustainable and effective solution by harnessing the power of green chemistry. We detail the synthesis of silver nanoparticles (AgNPs) using an extract from North Central Nigerian propolis, evaluating their performance as a corrosion inhibitor for carbon steel in a 1.0 M HCl solution. In this green approach, the propolis extract itself acts as both the reducing and stabilizing agent. The successful formation and characteristics of the resulting silver-propolis nanoparticles (Ag-PrNPs) were confirmed using a suite of analytical techniques, including UV-Visible Spectroscopy (UV-Vis), Fourier Transform Infrared Spectroscopy (FTIR), X-ray Diffraction (XRD), and advanced microscopy (SEM/EDX and STEM). To test their real-world effectiveness, we assessed corrosion inhibition through weight loss measurements at different temperatures and immersion times, as well as through electrochemical methods like potentiodynamic polarization (PDP) and electrochemical impedance spectroscopy (EIS). The results are highly promising: the Ag-PrNPs act as a powerful corrosion inhibitor, achieving an efficiency of over 96% in gravimetric tests. Our electrochemical data reveal that the inhibitor functions as a mixed-type inhibitor, suppressing both the anodic and cathodic reactions of corrosion. The formation of a protective film on the steel surface was confirmed by a significant increase in charge transfer resistance. We found that the inhibitor's adsorption onto the steel surface follows the Langmuir adsorption isotherm, and our thermodynamic analysis points to a spontaneous and exothermic adsorption process. This work successfully demonstrates a novel, eco-friendly, and highly effective strategy for mitigating steel corrosion using a readily available natural resource.

**Keywords:** Green corrosion inhibitor, Silver nanoparticles, Propolis, Carbon steel, Acid corrosion, Electrochemical impedance spectroscopy, Potentiodynamic polarization, Langmuir isotherm, Thermodynamic parameters, Green synthesis.

---

**INTRODUCTION**

In our modern world, we rely heavily on carbon steel. As the backbone of countless industries—from construction and automotive to manufacturing and energy—it accounts for about 85% of all steel produced annually [1, 2]. Yet, for all its strengths and affordability, carbon steel has a fundamental weakness: it is highly prone to corrosion, a natural electrochemical process that causes it to degrade when exposed to the elements [3]. The economic toll of this degradation is staggering, with global costs soaring past \$2.5 trillion each year. This figure represents more than just the price of replacing rusted parts; it includes the cascading costs of plant shutdowns, reduced operational efficiency, and the environmental impact of material failure

[3].

The problem becomes particularly acute in acidic environments. Industrial processes like acid pickling, large-scale cleaning, and oil well acidizing routinely expose carbon steel to highly corrosive acids that accelerate its decay [6]. For decades, the primary defense has been the use of corrosion inhibitors. However, the most common synthetic inhibitors, while effective, often come with a hidden cost: many are toxic, persist in the environment, and pose risks to ecosystems and human health. This has led to stricter regulations and a global search for safer, more sustainable alternatives [5].

This search has increasingly turned to "green" inhibitors—solutions derived from natural, renewable sources. These

materials offer the compelling advantages of being biodegradable, non-toxic, and environmentally friendly. A wealth of research has already shown that extracts from various plants can act as potent corrosion inhibitors for steel [1, 7, 34, 36]. Their effectiveness lies in their complex mixture of phytochemicals, such as alkaloids, tannins, and flavonoids. These molecules are rich in heteroatoms (like N, O, and S) and  $\pi$ -electrons, which allow them to readily adsorb onto a metal surface and form a protective shield against corrosive agents [7].

Among these natural sources, propolis stands out as a particularly promising candidate. This resinous substance, created by honeybees from plant materials, is a complex cocktail of polyphenols, flavonoids, and essential oils [8]. While famous for its medicinal properties [9], the very molecular features that make it a powerful antioxidant also make it an excellent corrosion inhibitor [2, 28].

Now, by merging the potential of this natural inhibitor with the cutting edge of nanotechnology, we can unlock even greater performance. Nanomaterials, with their incredibly high surface-area-to-volume ratio, can dramatically boost the effectiveness of inhibitor formulations [12]. Silver nanoparticles (AgNPs) are especially interesting due to their inherent stability and well-known antimicrobial properties [11]. When combined with an organic inhibitor like propolis, they can create a synergistic nanocomposite film. The organic molecules form the initial adsorbed layer, while the nanoparticles can physically block microscopic pits and defects on the steel surface, creating a much more robust barrier [13, 15].

Excitingly, these nanoparticles can be synthesized using green methods that align perfectly with our sustainability goals. By using the propolis extract itself as the reducing and capping agent, we can create AgNPs without resorting to harsh chemicals or energy-intensive processes [10, 17, 18, 19, 22, 23].

In this study, we present a comprehensive investigation into this promising approach. Our goal was to synthesize a novel silver-propolis nanocomposite (Ag-PrNPs) using propolis from North Central Nigeria and to rigorously test its ability to protect carbon steel in a highly corrosive 1.0 M HCl solution. Through a combination of gravimetric analysis, advanced electrochemical techniques, and detailed surface characterization, we aimed to not only measure its effectiveness but also to understand the underlying mechanisms of inhibition and adsorption.

## MATERIALS AND METHODS

### 2.1. Materials and Sample Preparation

Our investigation utilized carbon steel (CS) sheets (0.12 cm thick) with a standard industrial composition. For weight loss studies, we cut the sheets into 3 cm  $\times$  2 cm coupons. For the electrochemical tests, we embedded steel rods in epoxy resin, leaving a consistent working surface area of 1

cm<sup>2</sup>. To ensure a uniform and reactive surface for each experiment, we meticulously prepared the steel samples by abrading them with a series of silicon carbide (SiC) papers (from 400 to 1200 grit). After polishing, the samples were rinsed with double-distilled water, degreased with acetone, and dried before being stored in a desiccator to prevent any premature oxidation [14]. The corrosive test environment, a 1.0 M HCl solution, was prepared by diluting analytical grade hydrochloric acid.

### 2.2. Preparation of the Propolis Extract

To create our green inhibitor, we began by preparing an extract from locally sourced raw propolis from Benue State, North Central Nigeria. The raw material was first air-dried for two weeks and then ground into a fine powder. To remove any fatty components, a 100 g portion of the powder was first macerated in n-hexane for 72 hours. After filtering, the remaining solid material (the marc) was re-extracted with methanol for another 72 hours. This methanolic solution, containing the desired active compounds, was then concentrated using a rotary evaporator. The process yielded a viscous, dark-brown methanolic extract of propolis (NCNPE), which we stored in a cool, dark place until needed.

### 2.3. Green Synthesis of Silver-Propolis Nanoparticles (Ag-PrNPs)

The synthesis of our nanocomposite inhibitor was carried out using a straightforward green chemistry approach [18]. We first prepared a stock solution of the propolis extract in deionized water (1.0 g/100 mL). To this, we added an equal volume of 1.0 mM aqueous silver nitrate (AgNO<sub>3</sub>). The mixture was then stirred continuously in the dark for 48 hours. During this time, the biomolecules in the propolis extract acted as natural reducing agents, converting the silver ions (Ag<sup>+</sup>) into elemental silver (Ag<sup>0</sup>). The same molecules also served as capping agents, wrapping around the newly formed nanoparticles to prevent them from clumping together. The successful formation of AgNPs was signaled by a distinct color change in the solution to a stable yellowish-brown. The final nanoparticle suspension was then centrifuged to harvest the Ag-PrNPs pellets, which were washed and prepared for characterization and testing.

### 2.4. Characterization of the Nanocomposite

To understand the properties of our newly created Ag-PrNPs, we employed a range of analytical techniques.

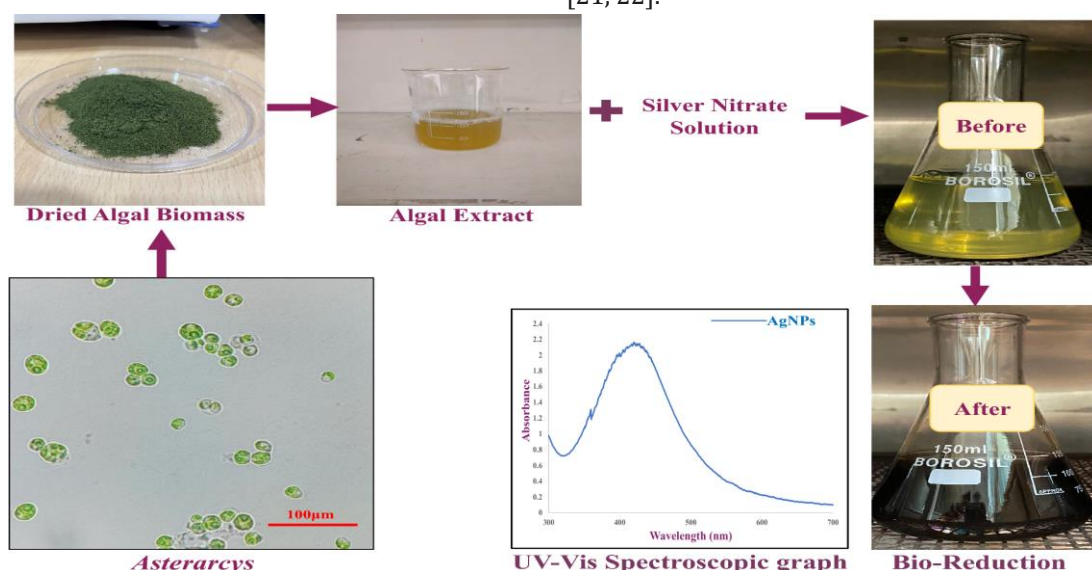
- **UV-Visible (UV-Vis) Spectroscopy:** We used a JENWAY 6405 UV-Vis spectrophotometer to confirm the formation of AgNPs. By scanning the solution from 300 to 700 nm, we looked for the tell-tale Surface Plasmon Resonance (SPR) peak that is characteristic of silver nanoparticles [21].
- **Fourier Transform Infrared (FTIR) Spectroscopy:** An Agilent Cary 630 FTIR spectrometer helped us identify which functional groups within the propolis

extract were responsible for reducing and stabilizing the nanoparticles.

- **X-ray Diffraction (XRD):** To confirm the crystalline nature of the silver in our composite, we used a Thermo Scientific ARL'XTRA X-ray diffractometer.
- **Scanning Electron Microscopy (SEM) and Energy Dispersive X-ray (EDX):** A Phenom Pro SEM allowed us to visualize the surface morphology of the Ag-PrNPs. Coupled with EDX, this technique also confirmed the elemental makeup of the composite, ensuring silver was present [24, 26].
- **Scanning Transmission Electron Microscopy (STEM):** For a more detailed, high-resolution view of the nanoparticles' size, shape, and distribution within the propolis matrix, we used a GeminiSEM-500-70-18 STEM [25].

### 2.5. Corrosion Inhibition Studies

- **Gravimetric (Weight Loss) Method:** This classic method involved immersing pre-weighed carbon steel coupons in the 1.0 M HCl solution, both with and without the Ag-PrNPs inhibitor at concentrations ranging from 200 to 1000 ppm. We ran two sets of experiments: one to study the effect of immersion time over 168 hours at room temperature, and another to study the effect of temperature (303 to 333 K) over a fixed 3-hour period. After immersion, the coupons were cleaned, dried, and reweighed to determine the amount of material lost to corrosion. From this data, we calculated the corrosion rate (CR) and inhibition efficiency (IE%) [19, 27].
- **Electrochemical Measurements:** For a more dynamic look at the inhibition process, we used a standard three-electrode electrochemical cell.
  - **Potentiodynamic Polarization (PDP):** These tests allowed us to see how the inhibitor affected both the anodic and cathodic reactions of corrosion. By scanning the potential around the



open circuit potential, we generated Tafel plots from which we could extract key corrosion parameters like corrosion current density ( $i_{corr}$ ) [30, 31, 38].

- **Electrochemical Impedance Spectroscopy (EIS):** EIS is a powerful non-destructive technique that provides insight into the properties of the protective film. By applying a small AC signal over a wide frequency range, we could measure the impedance of the steel surface. The resulting data, presented as Nyquist and Bode plots, allowed us to determine parameters like the charge transfer resistance ( $R_{ct}$ ), which is a direct measure of the corrosion resistance [4, 32].

### 2.6. Surface Analysis

To get a clear visual picture of the inhibitor's effectiveness, we used SEM to examine the surface of the carbon steel coupons after they had been immersed for 168 hours in the acid, both with and without the inhibitor. This allowed us to directly compare the protected surface to the severely corroded one [29].

## RESULTS AND DISCUSSION

### 3.1. Characterization of Synthesized Ag-PrNPs

#### 3.1.1. UV-Vis and FTIR Analysis

The first clue that our green synthesis was successful came from a distinct color change in the reaction mixture, which shifted from a light yellow to a stable, rich yellowish-brown. This visual cue, attributed to the Surface Plasmon Resonance (SPR) effect in nanoparticles, was definitively confirmed by UV-Vis spectroscopy [17]. The analysis revealed a strong, broad absorption peak centered around 422-435 nm, a hallmark signature of spherically shaped silver nanoparticles, providing clear evidence of their formation [21, 22].

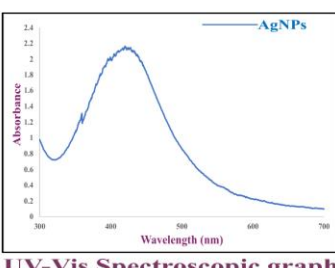


**Figure 1:** Schematic representation of the green synthesis of silver-propolis nanoparticles (Ag-PrNPs). The process involves (A) preparing a methanolic extract from raw propolis, (B) mixing the extract with an aqueous silver nitrate solution, resulting in (C) a visual color change from light yellow to yellowish-brown, indicating the bioreduction of  $\text{Ag}^+$  ions. This is confirmed by (D) the characteristic Surface Plasmon Resonance (SPR) peak observed in the UV-Vis spectrum.

To understand which components of the propolis were doing the work, we turned to FTIR spectroscopy. The spectrum of the pure propolis extract showed a variety of functional groups characteristic of polyphenolic compounds like flavonoids: a broad O-H stretch ( $\sim 3400 \text{ cm}^{-1}$ ), a C=O stretch ( $\sim 1700 \text{ cm}^{-1}$ ), and aromatic C=C stretches (1600-1450  $\text{cm}^{-1}$ ). When we analyzed the final Ag-PrNPs composite, we saw noticeable shifts and a decrease in the intensity of these O-H and C=O bands. This strongly suggests that these polyphenolic compounds were the key players, first acting as reducing agents to create the nanoparticles and then as capping agents, wrapping around the silver to provide stability [15].

### 3.1.2. XRD and STEM Analysis

Having confirmed the creation of our nanocomposite, we next sought to understand its structure. XRD analysis revealed sharp Bragg reflection peaks corresponding to the (111), (200), and (220) planes of silver, a pattern that is the fingerprint of silver's face-centered cubic (fcc) crystalline structure. This confirmed that our green synthesis produced genuinely crystalline metallic silver. Using the Debye-Scherrer equation, we calculated the average crystallite size to be approximately 2.36 nm [22].

For a closer look, STEM analysis provided high-resolution images. These images showed that the nanoparticles were mostly spherical or oval and were distributed quite uniformly throughout the organic propolis matrix. This

homogeneous distribution is a testament to the effectiveness of the propolis biomolecules as capping agents, successfully preventing the nanoparticles from clumping together into large, ineffective aggregates [24, 25].

### 3.1.3. SEM and EDX Analysis

SEM images gave us a broader view of the composite's morphology, showing that the Ag-PrNPs formed roughly spherical agglomerates. To confirm the composition, we used EDX, which detected a strong signal for silver (Ag), alongside the expected signals for carbon (C) and oxygen (O) from the propolis biomolecules. This combination of visual and elemental data verified that we had successfully created a true silver-propolis nanocomposite material [26].

## 3.2. Corrosion Inhibition Studies

### 3.2.1. Gravimetric Measurements: Effect of Concentration and Immersion Time

Our weight loss experiments clearly demonstrated the protective power of the Ag-PrNPs. As we increased the concentration of the inhibitor, the inhibition efficiency (IE%) rose dramatically, as summarized in Table 1. After a full 168 hours of immersion, the efficiency reached an impressive 96.44% at a concentration of 1000 ppm. This trend suggests that a higher concentration allows more inhibitor molecules to adsorb onto the steel, leading to more complete surface coverage and a stronger, more effective protective barrier against the acid [7, 34].

**Table 1: Inhibition Efficiency (IE%) from Gravimetric Measurements at Different Concentrations and Immersion Times.**

Time (hrs)	IE% at 200 ppm	IE% at 400 ppm	IE% at 600 ppm	IE% at 800 ppm	IE% at 1000 ppm
24	68.77	71.43	73.33	74.07	74.73
48	70.74	72.97	75.67	78.01	78.59
72	71.63	74.55	76.06	78.32	78.81
96	78.33	81.76	83.71	84.32	85.09
120	81.44	82.09	87.93	84.43	85.77
144	87.83	87.97	89.44	89.67	91.17
168	89.67	90.79	91.00	95.06	96.44

**3.2.2. Gravimetric Measurements: Effect of Temperature**

When we investigated the effect of temperature, we found that the inhibitor's efficiency decreased as the temperature rose (Table 2). For instance, the high efficiency of over 91% seen at 303 K (30°C) for the 1000 ppm concentration

dropped to around 60% at 333 K (60°C). This behavior suggests that the protective film may be partially held together by physical adsorption (physisorption), where the bonds are weaker and can be disrupted by increased thermal energy, causing some inhibitor molecules to desorb from the surface [31].

**Table 2: Effect of Temperature on Inhibition Efficiency (IE%) from Gravimetric Measurements (3-hour immersion).**

Temperatur e (K)	IE% at 200 ppm	IE% at 400 ppm	IE% at 600 ppm	IE% at 800 ppm	IE% at 1000 ppm
303	60.68	65.09	76.15	82.24	91.63
313	58.66	58.93	61.57	63.21	67.67
323	57.13	57.11	61.00	62.28	64.54
333	54.87	56.56	57.25	59.78	60.47

**3.3. Electrochemical Studies**
**3.3.1. Potentiodynamic Polarization (PDP)**

The PDP results provided deeper insight into how the inhibitor works. The Tafel plots showed that adding the Ag-PrNPs suppressed the rate of both the anodic reaction (the dissolution of iron) and the cathodic reaction (the

evolution of hydrogen gas). Key parameters extracted from these plots are shown in Table 3. Because the corrosion potential (Ecorr) did not shift significantly (less than 85 mV), we can classify the Ag-PrNPs as a mixed-type inhibitor—it doesn't just block one pathway but rather interferes with the overall corrosion process by acting on both anodic and cathodic sites [6, 31, 38].

**Table 3: Potentiodynamic Polarization Parameters for Carbon Steel in 1.0 M HCl.**

Concentratio n (ppm)	Ecorr (mV vs SCE)	icorr ( $\mu\text{A}/\text{cm}^2$ )	$\beta_a$ (mV/dec)	$\beta_c$ (mV/dec)	IE%
Blank	-475	1150	75	-118	-
200	-482	483	79	-120	58.0
400	-488	322	81	-122	72.0
600	-495	196	84	-125	82.9
800	-501	127	88	-128	88.9
1000	-506	81	92	-130	92.9

### 3.3.2. Electrochemical Impedance Spectroscopy (EIS)

EIS measurements offered a powerful way to characterize the protective film. The Nyquist plots for the uninhibited steel showed a small semicircle, indicating low resistance to corrosion. As we added the inhibitor, the diameter of this semicircle grew dramatically. This diameter represents the charge transfer resistance ( $R_{ct}$ ), and its substantial increase, detailed in Table 4, is direct evidence of the formation of a highly effective insulating barrier on the

steel surface that slows down the corrosion process [4, 12]. The semicircles were not perfect, a common phenomenon known as frequency dispersion, which is due to the inherent roughness and inhomogeneity of the steel surface [26]. The corresponding decrease in the double-layer capacitance ( $C_{dl}$ ) with increasing inhibitor concentration further supports this picture, as the adsorbed organic molecules displace water at the interface, thickening the electrical double layer [32].

**Table 4: Electrochemical Impedance Spectroscopy (EIS) Parameters for Carbon Steel in 1.0 M HCl.**

Concentration (ppm)	$R_{ct}$ ( $\Omega \cdot \text{cm}^2$ )	n	$C_{dl}$ ( $\mu\text{F}/\text{cm}^2$ )	IE%
<b>Blank</b>	11.6	0.88	934	-
<b>200</b>	27.3	1.00	752	57.5
<b>400</b>	33.7	0.89	269	65.6
<b>600</b>	45.9	0.92	133	74.7
<b>800</b>	59.1	0.86	102	80.4
<b>1000</b>	86.0	0.87	70	86.5

### 3.4. Adsorption Isotherm and Thermodynamic Parameters

#### 3.4.1. Adsorption Isotherm

To model the interaction between our inhibitor and the steel, we tested several adsorption isotherm models. The data fit best with the Langmuir adsorption isotherm, which assumes that the inhibitor forms a single, uniform layer (a monolayer) on the steel surface. The strong linear fit ( $R^2$  values close to 1), as shown in Table 5, supports this model, suggesting that the inhibitor molecules occupy specific active sites on the metal until the surface is covered [1, 37].

#### 3.4.2. Thermodynamic Parameters

By analyzing the effect of temperature on the corrosion

rates, we calculated key thermodynamic parameters. We found that the activation energy ( $E_a$ ) for corrosion was higher in the presence of the inhibitor, confirming that the adsorbed film acts as an energy barrier that makes corrosion more difficult to initiate. The calculated standard free energy of adsorption ( $\Delta G_{ads}^\circ$ ) was negative, indicating that the adsorption of the inhibitor onto the steel surface is a spontaneous process. The magnitude of this value suggests a comprehensive adsorption mechanism that involves a combination of both physical forces (physisorption) and the formation of chemical bonds (chemisorption) between the inhibitor molecules and the iron atoms of the steel [35, 36]. The key thermodynamic and adsorption parameters are summarized in Table 5.

**Table 5: Thermodynamic and Langmuir Adsorption Parameters.**

Parameter	Blank	200 ppm	400 ppm	600 ppm	800 ppm	1000 ppm

Ea (kJ/mol)	14.68	33.31	36.07	39.66	46.30	54.00
$\Delta H^\circ_{\text{ads}}$ (kJ/mol)	-11.97	-30.61	-33.36	-36.95	-43.59	-51.29
$\Delta S^\circ_{\text{ads}}$ (J/mol·K)	-199.7	-161.9	-154.1	-143.8	-124.5	-101.9
$\Delta G^\circ_{\text{ads}}$ (kJ/mol at 303K)	-	-23.8	-25.1	-26.5	-28.1	-29.9
Langmuir R <sup>2</sup> (at 303K)	-	0.991	0.993	0.995	0.992	0.991

### 3.5. Surface Morphology Analysis

A picture is worth a thousand words, and the SEM images of the steel coupons after the experiment provided striking visual proof of the inhibitor's effectiveness. The coupon exposed to the acid without any protection was a landscape of destruction—rough, pitted, and severely corroded. In stark contrast, the coupon protected by our Ag-PrNPs inhibitor was remarkably smooth and almost entirely free of corrosion damage. This provides direct, visual confirmation of the formation of a stable and highly protective film [16, 29].

## CONCLUSION

In this comprehensive study, we have successfully developed a novel, eco-friendly corrosion inhibitor by synthesizing silver nanoparticles within a natural propolis matrix. Our findings clearly establish its exceptional performance in protecting carbon steel from aggressive acid attack. The key takeaways from our research are:

1. We demonstrated a simple and effective one-pot green synthesis for creating a stable silver-propolis nanocomposite (Ag-PrNPs), confirmed through extensive material characterization.
2. The Ag-PrNPs composite proved to be an outstanding corrosion inhibitor, achieving over 96% efficiency in weight loss tests and showing strong performance in electrochemical evaluations.
3. Our electrochemical data revealed that the composite acts as a mixed-type inhibitor, forming a robust protective film that significantly impedes the corrosion process.
4. The adsorption of the inhibitor onto the steel surface is a spontaneous process that follows the Langmuir isotherm, indicating the formation of a protective

monolayer.

5. The mechanism appears to be a comprehensive one, involving both physisorption and chemisorption, which creates a durable barrier against corrosion.

Ultimately, this research highlights a powerful and sustainable strategy for corrosion protection. By combining the inherent inhibitory properties of a natural resource like propolis with the unique advantages of nanotechnology, we can create next-generation materials that are not only highly effective but also environmentally responsible.

## REFERENCES

1. G.A. Ijuo, M. A. Orokpo, N. Surma, P.N Tor, "Methanol extract of *Canarium Sweinfurthii* as a green inhibitor for the corrosion of mild steel in HCl: adsorption, kinetic, thermodynamic and synergistic studies" *J. Mater. Environ. Sci.*, 2018, 9, 11, 3113-3123.
2. A. M. Orokpo, R. A. Wuana, H.F. Chuhul, I.S. Eneji, "Corrosion Inhibition Potential of Benue Propolis Extracts on Carbon Steel in 1.0 M Hydrochloric Acid Medium: Experimental and Computational Studies," *Progress in Chemical and Biochemical Research* 2022, 5, 3, 283-300.
3. F. George, P.E. Hays, "International Symposium on Corrosion for Sustainable development, World Corrosion Organization, 2022.
4. L. T. Popoola, A. S. Yusuff, O. M. Ikumapayi, O. M. Chima, A. T. Ogunyemi, B. A. Obende, "Electrochemical, Isotherm, and Material Strength Studies of *Cucumeropsis mannii* Shell Extract on A515 Grade 70 Carbon Steel in NaCl Solution," *Hindawi International Journal of Corrosion*, 2022, 3189844, 22, <https://doi.org/10.1155/2022/3189844>.
5. B. R. Fazal, T. Becker, B. Kinsella, and K. Lepkova, "A

## EUROPEAN FRONTIERS IN CURRENT SCIENCE AND RESEARCH

review of plant extracts as green corrosion inhibitors for CO<sub>2</sub> corrosion of carbon steel," *npj Materials Degradation*, 2022, 6.

6. A. S. Fouad1, H. S. El-Desoky, M. A. Abdel-Galeil, D. Mansour, "Niclosamide and dichlorphenamide: new and effective corrosion inhibitors for carbon steel in 1M HCl solution" *SN Applied Sciences*, 2021, 3, 287, <https://doi.org/10.1007/s42452-021-04155-w>.

7. C. C. Aralu, H. O. Chukwuemeka-Okorie, K. G. Akpomie, "Inhibition and adsorption potentials of mild steel corrosion using methanol extract of *Gongronema latifolium*," *Applied Water Science*, 2021, 11, 22 <https://doi.org/10.1007/s13201-020-01351-8>.

8. V.D. Wagh "Propolis, a wonder bees product and its pharmacological potentials" *Adv Pharmacol Sci*, 2013, 308249.

9. G.A. Burdock, "Review of the biological properties and toxicity of bee propolis" *Food and Chemical Toxicology*; 1998, 36, 347–363.

10. S. Patil, N. Desai, K. Mahadik, A. Paradkar, "can green synthesized propolis loaded silver nanoparticulate gel enhance wound healing caused by burns?" *European Journal of Integrative Medicine*, 2015, S1876-3820, 00043-8, <http://dx.doi.org/10.1016/j.eujim.2015.03.002>.

11. D. Nayak, S. Ashe, P.R. Rauta, "Bark extract mediated green synthesis of silver nanoparticles: Evaluation of antimicrobial activity and antiproliferative response against osteosarcoma" *Mater Sci Eng*, 2016, 58, 44–52.

12. T.W. Quadri, L.O. Olasunkanmi, O.E. "Fayemi, Zinc oxide nanocomposites of selected polymers: synthesis, characterization, and corrosion inhibition studies on mild steel in HCl solution" *ACS Omega*, 2017, 2, 8421–8437.

13. M.M. Solomon, H. Gerengi, S.A. Umoren, "Gum Arabic – silver nanoparticles composite as a green anticorrosive formulation for steel corrosion in a strong acid media," *Carbohyd Polym*, 2018, 181, 43–55.

14. T.B. Asafa, M.O. Duwoju, K.P. Madingwaneng, S. Diouf, E.R. Sadiku, M.B Shongwe, P.A. Olubami, O.S. Ismail. M.T. Ajala and K.O. Oladosun, "Gr-Al composite reinforced with Si<sub>3</sub>N<sub>4</sub> and SiC particles for enhanced microhardness and reduced thermal expansion," *Appl. Sci.* 2020, 1026. <https://doi.org/10.1007/s42452-020-2838-5>.

15. G. A. Ijue, S. Nguamo, J. O. Igoli, "Ag-nanoparticles Mediated by *Lonchocarpus laxiflorus* Stem Bark Extract as Anticorrosion Additive for Mild Steel in 1.0 M HCl Solution," *Progress in Chemical and Biochemical Research* 2022, 5, 2, 133-146.

16. O.A. Odewole, C.U. Ibeji, H.O. Oluwasola, O.E. Oyeneyin, K.G. Akpomie, C.M. Ugwu, C.G. Ugwu, T.E. Bakare, "Synthesis and anti-corrosive potential of Schiff bases derived 4-nitrocinnamaldehyde for mild steel in HCl medium: experimental and DFT studies". *J Mol Struct*, 2021, 1223:129214.

17. H. P. Meena, A. P. Singh, and K. K. Tejavath, "Biosynthesis of Silver Nanoparticles Using *Cucumis prophetarum* Aqueous Leaf Extract and Their Antibacterial and Antiproliferative Activity Against Cancer Cell Lines", *ACS OMEGA*, 2020, 5, 5520–5528, <https://dx.doi.org/10.1021/acsomega.0c00155>.

18. K. Shameli, M. Bin Ahmad, E.A.J. Al-Mulla, N.A. Ibrahim, P. Shabanzadeh, A. Rustaiyan, Y. Abdollahi, S. Bagheri, S. Abdolmohammadi, M.S. Usman, M. Zidan, "Green biosynthesis of silver nanoparticles using *Callicarpa maingayi* stem," *Molecules*, 2016, 8506-17. doi: 10.3390/molecules17078506.

19. M. Bilal, T. Rasheed, H.M. Iqbal, C. Li, H. Hu, X. Zhang, "Development of silver nanoparticles loaded chitosan-alginate constructs with biomedical potentialities," *Int. J. Biol. Macromol*, 2017, 105, 393–400.

20. G. M Srirangam, K. ParameswaraRao, "Synthesis and characterization of silver nanoparticles from the leaf extract of *Malachra capitata* (L)," *RJC*, 2017, 10, 1, 46-53.

21. V. Thiruvengadam, A.V. Bansod, "Characterization of Silver Nanoparticles Synthesized using Chemical Method and its Antibacterial Property," *Biointerface Research in Applied Chemistry*, 2020, 10, 6, 10.33263/BRIAC106.72577264.

22. P. Logeswari, S. Silambarasan, J. Abraham, "Synthesis of silver nanoparticles using plants extract and analysis of their antimicrobial property," *J Saudi Chem Soc*, 2015, 19:311–317.

23. L. S. Al Banna, N. M. Salem, G. A. Jaleel and A. M. Awwad, "Green synthesis of sulfur nanoparticles using *Rosmarinus officinalis javanica* leaves extract and nematicidal activity against *Meloidogyne*," *Chemistry International*, 2020, 6, 3.

24. J. Liu, "Advances and Applications of Atomic-Resolution Scanning Transmission Electron Microscopy," *Microscopy and Microanalysis* 2021, 27, 943–995 doi:10.1017/S1431927621012125.

25. S. V. Kalinin, C. Ophus, P. M. Voyles, R. Erni, D. Kepaptsoglou, V. Grillo, A. R. Lupini, M. P. Oxley, E. Schwenker, M. K. Y. Chan, J. Etheridge, X. Li, G. G. D. Han, M. Ziatdinov, N. Shibata, S. J. Pennycook, "Machine learning in scanning transmission electron microscopy," *Nature Reviews Methods Primers*, 2022, 2, 1, 10.1038/s43586-022-00095-w.

26. V.O. Kharlamov, Aleksandr Vasilevich Krokhalev, S.V. Kuz'min, V.I. ysak, "Investigation of the Structure and Distribution of Chemical Elements between the Phases of Hard Alloys of the Cr<sub>3</sub>C<sub>2</sub>-Ti System, Obtained at Various Modes of Explosive Compaction," *Materials Science Forum*, 2020, 992, 487-492, 10.4028/www.scientific.net/MSF.992.487.

27. G. A. Ijue, A. M. Orokpo, P. N. Tor, "Effect of Spondias

## EUROPEAN FRONTIERS IN CURRENT SCIENCE AND RESEARCH

mombin Extract on the Corrosion of Mild Steel in Acid Media," Chemistry Research Journal, 2018, 3, 3, 64-77.

28. A. M. Orokpo, R. A. Wuana, H.F. Chuhul, I.S. Eneji, "Corrosion Inhibition Potential of Benue Propolis Extracts on Carbon Steel in 1.0 M Hydrochloric Acid Medium: Experimental and Computational Studies," Progress in Chemical and Biochemical Research 2022, 5, 3, 283-300.

29. E. Ituen, L. Yuanhua, C. Verma, A. Alfantazi, O. Akaranta, E. E. Ebenso, "Synthesis and characterization of walnut husk extract-silver nanocomposites for removal of heavy metals from petroleum wastewater and its consequences on pipework steel corrosion," Journal of Molecular Liquids, 2021, 335, 116132, doi.org/10.1016/j.molliq.2021.116132.

30. H.F.Chahul, C.O. Akalezi, A.M. Ayuba, "Effect of adenine, guanine and hypoxanthine on the corrosion of mild steel in H<sub>3</sub>PO<sub>4</sub>. International Journal of Chemical Science," 2015, 7, 2006-3350.

31. A. Akpan, N.O. Offiong, "Electrochemical linear polarization studies of Amodiaquine drug as a corrosion inhibitor for mild steel in 0.1M HCl solution," Chem Mater Res, 2015, 7, 17-20.

32. M. H. Nazari, M. S. Shihab, L. Cao, E. A. Havens, and X. Shi, "A peony-leaves-derived liquid corrosion inhibitor: protecting carbon steel from NaCl," Green Chemistry Letters and Reviews, 2017, 10, 4, 359-379.

33. M. H. Nazari, M. S. Shihab, E. A. Havens, and X. Shi, "Mechanism of corrosion protection in chloride solution by an applebased green inhibitor: experimental and theoretical studies," Journal of Infrastructure Preservation and Resilience, 2020, 1, 7.

34. N. B. Iroha, N. J. Maduelosi, "Corrosion Inhibitive Action and Adsorption Behaviour of *Justicia Secunda* Leaves Extract as an Eco-Friendly Inhibitor for Aluminium in Acidic Media" 2021, 11, 13019 - 13030, doi.org/10.33263/BRIAC115.1301913030.

35. A.I. Ali, Y.S. Mahrousb, "Corrosion inhibition of C-steel in acidic media from fruiting bodies of *Melia azedarach* L extract and a synergistic Ni<sup>2+</sup> additive", RSC Adv. 2017, 7, 23687-23698.

36. N.AI Otaibi, H.H. Hammud, Corrosion Inhibition Using Harmal Leaf Extract as an Eco-Friendly Corrosion Inhibitor, Molecules, 26(2021) 7024, <https://doi.org/10.3390/molecules26227024>.

37. G.A. Ijuo, H.F. Chahul, and I.S. Eneji, Corrosion inhibition and adsorption behavior of *Lonchocarpus laxiflorus* extract on mild steel in hydrochloric acid. Ew J Chem Kinet 2016, 1, 21-30.

38. S. Ibrahim, R. Sanmugapriya, J. A. Selvi, T. P. Malini, P. Kamaraj, P. A. Vivekanand, G. Periyasami, A. Aldalbahi, K. Perumal, J. Madhavan, and S. Khanal, "Effect of 3-Nitroacetophenone on Corrosion Inhibition of Mild Steel in Acidic Medium," 2022, 2022, <https://doi.org/10.1155/2022/727667>.